Dyes and Pigments 95 (2012) 373–376

Contents lists available at SciVerse ScienceDirect

Dyes and Pigments

journal homepage: www.elsevier.com/locate/dyepig

Quinoline-based fluorescent probe for ratiometric detection of hydrogen peroxide in aqueous solution

Yuan-Yu Qian [a,*], Lin Xue [b], De-Xin Hu [c], Guo-Ping Li [b], Hua Jiang [b,**]

[a] Emergency Department of Chinese PLA General Hospital, Beijing 100853, PR China
[b] Beijing National Laboratory for Molecular Sciences, CAS Key Laboratory of Photochemistry, Institute of Chemistry, Chinese Academy of Sciences, Beijing 100190, PR China
[c] Chemicals, Minerals & Metallic Materials Inspection Center, Tianjin Entry-Exit Inspection & Quarantine Bureau, Tianjin 300456, PR China

ARTICLE INFO

Article history:
Received 28 February 2012
Received in revised form
12 May 2012
Accepted 14 May 2012
Available online 23 May 2012

Keywords:
Fluorescent probe
Hydrogen peroxide
Quinoline
Boronate cleavage
Protonation
Ratiometric

ABSTRACT

A novel quinoline-based fluorescent probe for detecting H_2O_2 is described. In aqueous solution, the probe exhibits fluorescence emission at 542 nm originating from the monocationic species. The reaction between the probe and H_2O_2 causes quenching of the emission at 542 nm and simultaneously yields a significant hypsochromic shift of the emission maximum to 480 nm due to the H_2O_2-triggered boronate cleavage process. Thus, a single-excitation, dual-emission ratiometric measurement with a large blue shift in emission ($\Delta\lambda = 62$ nm) and remarkable changes in the ratio ($F_{480\ nm}/F_{542\ nm}$) of the emission intensity (R/R_0 up to 8.3-fold) can be established. Moreover, the probe can also afford high selectivity for detecting H_2O_2 over other biological reactive oxygen species.

1. Introduction

The development of fluorescence imaging technology visualizing intracellular hydrogen peroxide (H_2O_2) has been attracting more and more attention, because H_2O_2, a by-product of oxygen metabolism, can accumulate in cells leading to oxidative stress and subsequent serious health problems [1]. Recent evidence has demonstrated that H_2O_2 is also a messenger in normal cellular processes [2]. Therefore, design of highly sensitive and selective H_2O_2 fluorescent probes will provide useful tools for intracellular H_2O_2 detection and further H_2O_2-biological studies. Although several fluorescent probes, such as 2′,7′-dichlorofluorescin [3], have already been used for H_2O_2 imaging, the chemoselectivity from other ROS/RNS (reactive oxygen or nitrogen species) was not satisfactory. In the few past years, owing to the intelligent design mechanisms and methods, including benzenesulfonyl ester [4], benzil [5], or boronate ester chemistry [6], fluorescent probes with improved sensitivity and selectivity have been constructed. Nevertheless, most of them are fluorescence intensity-based probes, and cannot provide sufficient accuracy for quantitative measurements, because the intracellular fluorescence may suffer from many sources of external interference. As an ideal solution, ratiometric probes can provide self-calibration via two selected emission wavelengths [7]. They are good candidates for accurate and quantitative analysis. However, few ratiometric probes for H_2O_2 have been achieved [8]; it is rather desirable to design ratiometric H_2O_2-selective probes.

To this end, we now report the synthesis and photophysical properties of a ratiometric probe (DQHP) for H_2O_2. As shown in Scheme 1, the boronate-based benzyl cleavable group was conjugated to the 4-position of 6-dimethylamino-2-methyl quinolinone (1). We anticipated that the probe can be protonated in neutral aqueous solution and form a charge delocalized state due to the resonance charge transfer from the oxygen atom to quinolinic nitrogen atom (Scheme 2) [9]. If H_2O_2 triggers the boronate cleavage to form compound 1 [6,8], the resonance will be shut down and a distinct emission maxima shift will also be observed.

2. Experiment procedure

2.1. General

All chemicals were purchased from Alfa Aesar or Sigma–Aldrich and used as received. All solvents were purified and dried by

* Corresponding author.
** Corresponding author. Tel./fax: +86 10 82612075.
E-mail addresses: qyy301@sina.com (Y.-Y. Qian), hjiang@iccas.ac.cn (H. Jiang).

0143-7208/$ – see front matter © 2012 Elsevier Ltd. All rights reserved.
doi:10.1016/j.dyepig.2012.05.013

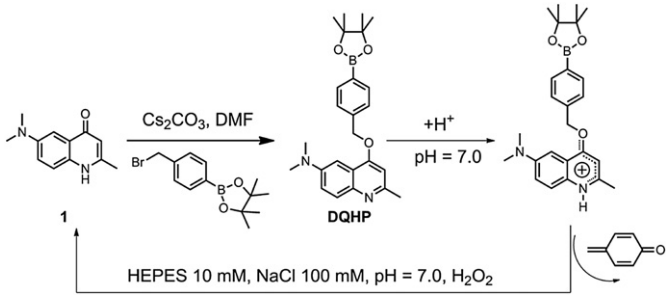

Scheme 1. Synthesis and action of probe DQHP.

standard methods prior to use. Pure water (18.2 Ω) was used to prepare all aqueous solutions. ^{1}H NMR and ^{13}C NMR spectra were recorded on a Bruker AVANCE-400 400 MHz spectrometer. All chemical shifts are reported in the standard notation of parts per million using residual solvent protons as internal standard. IR data were recorded on a Bruker Tensor-27 spectrometer. Mass spectra (ESI) were obtained on LC-MS 2010 mass spectrometer. All titrations were carried out in HEPES buffer (10 mM HEPES, 100 mM NaCl, pH = 7.0, 25 °C). UV–Vis absorption spectra were obtained using Shimadzu UV-2550 spectrometer. Fluorescence spectra were obtained using HITACHI F-4600 spectrometer. Various reactive oxygen species were obtained according to the typical procedures reported by Chang et al. [8,10].

2.2. Synthesis

Synthesis of Compound 3. A solution of compound 2 (1.0 g, 6 mmol), ethyl acetoacetate (1.6 g, 12 mmol), and AcOH (0.5 mL) in benzene (30 mL) was heated under reflux for 8 h, removing water with a Dean–Stark apparatus. This mixture was cooled to room temperature and concentrated in vacuum. The residue was purified by flash chromatography (silica gel, petroleum ether/0–10% ethyl acetate) to give the desired products as colourless oil (63%). TLC: R_f = 0.53 (silica, 5:1 petroleum ether/ethyl acetate). Mp: 69–70 °C. FTIR (KBr, cm^{-1}): 3271, 3032, 2991, 2915, 2803, 2305, 1652, 1613, 1521, 1488, 1437, 1387, 1351, 1263, 1159, 1058, 1020, 976, 947, 837, 784, 733, 688, 602, 555, 522, 492. ^{1}H NMR (400 MHz, $CDCl_3$, ppm): δ 10.08 (s, 1H), 6.99 (d, J = 8.44 Hz, 2H), 6.68 (br, 2H), 4.61 (s, 1H), 4.17 (q, J = 7.00 Hz, 2H), 2.94 (s, 6H), 1.87 (s, 3H), 1.30 (t, J = 7.12 Hz, 3H). ^{13}C NMR (100 MHz, $CDCl_3$, ppm): δ 170.7, 160.9, 148.8, 128.6, 126.9, 112.8, 84.0, 58.7, 40.9, 20.3, 14.8. (ESI): m/z Calcd for [M + H$^+$] $C_{14}H_{21}N_2O_2$: m/z 249.16. Found: m/z 249.2. Calcd for [M + Na$^+$] $C_{14}H_{20}N_2NaO_2$: m/z 271.44 Found: 271.2.

Synthesis of Compound 1. A mixture of compound 3 (0.74 g, 3 mmol) and diphenyl ether (10 mL) was heated with stirring at 250 °C for 60 min under nitrogen. This mixture was cooled, and the product began to precipitate in the reaction medium. After cooling, the mixture was diluted with petroleum ether (100 mL) to complete the precipitation. The solid was collected by filtration and recrystallized from methanol to give of the product as yellow crystals (0.44 g, 73%). Mp: >300 °C. TLC: R_f = 0.30 (silica gel, dichloromethane/0–2% methanol). FTIR (KBr, cm^{-1}): 3242, 3068, 2891, 2807, 2781, 1609, 1584, 1546, 1495, 1380, 1306, 1252, 1218, 1180, 1086, 964, 868, 823, 697, 617, 563, 498. ^{1}H NMR (400 MHz, DMSO-d_6, ppm): δ 11.3 (s, 1H), 7.39 (d, J = 9 Hz, 1H), 7.24–7.18 (m, 2H), 5.78 (s, 1H), 2.93 (s, 6H), 2.29 (s, 3H). ^{13}C NMR (100 MHz, MeOD, ppm): δ 179.7, 150.6, 149.4, 133.9, 126.4, 121.6, 119.9, 108.2, 105.2, 41.1, 19.7. (ESI): m/z Calcd for [M + H$^+$] $C_{12}H_{15}N_2O$: m/z 203.12. Found: m/z 203.1.

Synthesis of DQHP. A mixture of compound 1 (202 mg, 1 mmol), 4-(bromomethyl)benzeneboronic acid pinacol ester (356 mg, 1.2 mmol), and Cs_2CO_3 (490 mg, 1.5 mmol) in N,N-dimethylformamide (DMF; 15 mL) was heated at 80 °C for 8 h. After cooling, H_2O (30 mL) was added to the mixture and extracted with CH_2Cl_2 (10 mL × 3). The organic solutions were combined, washed with water and brine, and dried with Na_2SO_4. The solvents were evaporated to give the crude product, which was purified by flash chromatography (silica gel, dichloromethane/0–2% methanol) to give the desired products as a pale solid (0.24 g, 57%). TLC: R_f = 0.52 (silica, 25:2 CH_2Cl_2/MeOH). Mp: 149–150 °C. FTIR (KBr, cm^{-1}): 3423, 3031, 2979, 2925, 2803, 1620, 1594, 1564, 1511, 1451, 1397, 1357, 1324, 1271, 1246, 1219, 1191, 1143, 1093, 1014, 965, 886, 857, 826, 731, 707, 660, 604, 523, 438. ^{1}H NMR (400 MHz, $CDCl_3$, ppm): δ 7.87–7.83 (m, 3H), 7.52 (d, J = 7.8 Hz, 2H), 7.34 (m, 1H), 7.23 (d, J = 2.84 Hz, 1H), 6.58 (s, 1H), 5.30 (s, 2H), 3.04 (s, 6H), 2.61 (s, 3H), 1.36 (s, 12H) ^{13}C NMR (100 MHz, $CDCl_3$, ppm): δ 160.0, 155.6, 148.0, 142.8, 139.5, 135.2, 128.9, 126.5, 120.9, 119.4, 101.8, 100.2, 84.0, 69.9, 41.0, 25.7, 25.0. (ESI): m/z Calcd for [M + H$^+$] $C_{25}H_{32}BN_2O_3$: m/z 419.25. Found: m/z 419.4.

3. Results and discussions

As shown in Scheme 3, compound 1 was synthesized according to a typical procedure [9d]. The enamine 3 was obtained by condensation of the 4-dimethylaminoaniline with ethyl acetoacetate. Compound 3 was cyclized by heating in diphenyl ether under nitrogen to give quinolone 1 in 73% yield. O-alkylation using 4-(bromomethyl)benzeneboronic acid pinacol ester under basic conditions gave DQHP in moderate yield.

From the fluorimetric titration, the solubility of DQHP is about 15 μM in physiological buffer (10 mM HEPES, 100 mM NaCl, pH = 7.0), which is sufficient for spectral measurements or cellular staining (Fig. S1).

To evaluate whether our probe can be protonated under neutral conditions, we measured the fluorescence spectra of DQHP at various pH (pH below 5 or above 10 were not measured to avoid potential hydrolysis of pinacol ester, Fig. 1). The pK_a value of 7.47 ± 0.05 clearly indicates that probe DQHP has the similar protonation behaviour to the methylpropane-substituted analogues (Scheme 2) [9d]. Under neutral conditions, DQHP exhibited a clear absorption band around 400 nm (ε = 2.48 × 10^4 M^{-1} cm^{-1} measured at 405 nm, Fig. 2). Upon addition of 1 mM H_2O_2 for 90 min, this band gradually decreased with a concomitant increase around 346 nm. Meanwhile, the absorption spectrum of compound 1 also

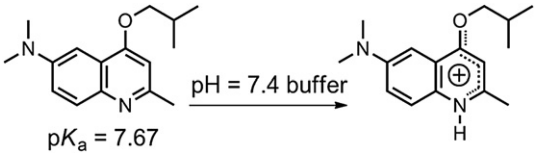

Scheme 2. The protonation and resonance of the 4-isobutoxy substituted quinoline.

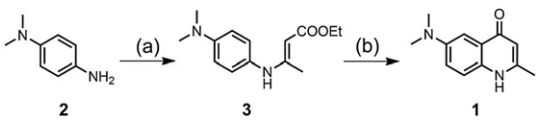

Scheme 3. Synthetic procedure for compound 1. (a) Ethyl acetoacetate, AcOH, benzene, reflux. (b) Diphenyl ether, 250 °C.

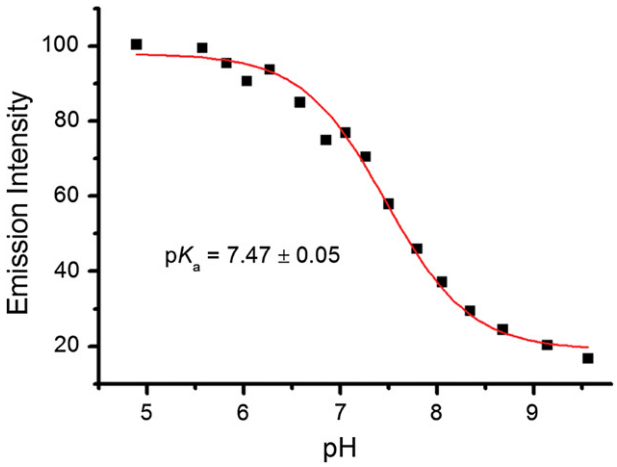

Fig. 1. Fluorescence emission intensity (λ_{em} = 540 nm) of DQHP (5 μM) over the pH range 5–9, the solid lines represent the non-linear least-squares fits to the experimental data.

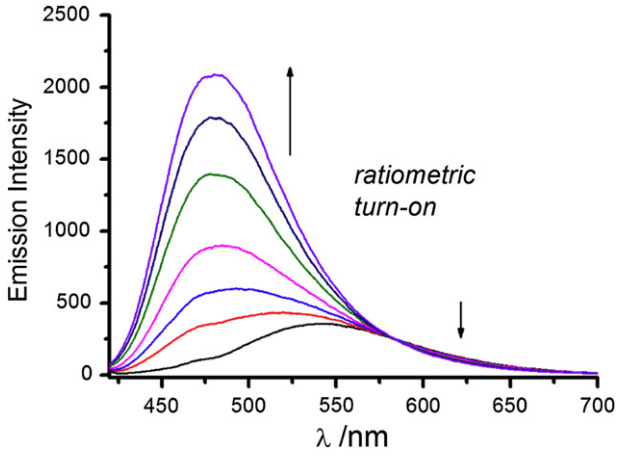

Fig. 3. Fluorescence emission spectra (λ_{ex} = 405 nm) of DQHP (5 μM) upon addition of H_2O_2 (100 μM) for 5, 15, 30, 60, 90, 120 min in HEPES buffer.

featured an aborption maximum at 346 nm, suggesting that the H_2O_2-triggered boronate cleavage process occurred [6,8]

Next we evaluated fluorescence emission property of DQHP (5 μM) in HEPES buffer (10 mM HEPES, 100 mM NaCl, pH = 7.0). When excited at 405 nm, DQHP displayed a weak fluorescence emission maximum at 542 nm (Φ = 0.07, Fig. 3), which is very similar to our previous observations with quinoline analogues [9d]. It clearly demonstrates the existence of the resonance charge transfer in the monoprotonated form of DQHP. When treating DQHP with 1 mM H_2O_2, the fluorescence showed remarkable enhancements (17.5-fold, measured at 480 nm) and the emission maximum gradually blue-shifted to 480 nm. Through measuring reaction product of compound 1, we found 1 is in the neutral form in HEPES buffer (Fig. S3). Its emission maximum and quantum yield were characterized to be 480 nm and 0.58, respectively. Under pseudo-first-order kinetics (1.25 μM DQHP, 1 mM H_2O_2), the observed rate constant for H_2O_2 deprotection is $k_{obs} = 1.40 \times 10^{-3}$ s^{-1} (Fig. 4). Therefore, it is clear that DQHP can respond to H_2O_2 with significant ratiometric and turn-on fluorescence signal output, and the ratios of the fluorescence intensities at 480 and 542 nm were found to be 0.34 and 2.82 in the absence and presence of H_2O_2, respectively, (R/R_0 = 8.3). These data imply DQHP is a good candidate for ratiometric and turn-on detection of H_2O_2 in aqueous solution because of the large emission shift (62 nm) and ratio changes.

In addition, the chemoselectivity profile of DQHP for H_2O_2 was investigated by fluorimetric titration of different ROS (Fig. 5). As expected, only H_2O_2 significantly increases the emission ratio ($F_{480}/F_{542\ nm}$). But in the presence of other ROS, including tert-butylhydroperoxide (TBHP), hypochlorite (ClO^-), hydroxyl radical ($^{\bullet}OH$), tert-butoxy radical ($^{\bullet}O^tBu$), nitric oxide (NO), and superoxide ($O_2^{\bullet-}$), no evident fluorescence emission ratio changes were observed. Thus, DQHP also has excellent chemoselectivity for H_2O_2 over other competing ROS. Furthermore, the emission ratio of both DQHP and compound 1 displayed pH insensitivity over biological window of 5.5–8 (Fig. S4). That implies subtle pH changes do not interfere with the ratiometric detection of H_2O_2 under physiological conditions. In addition, it has been shown

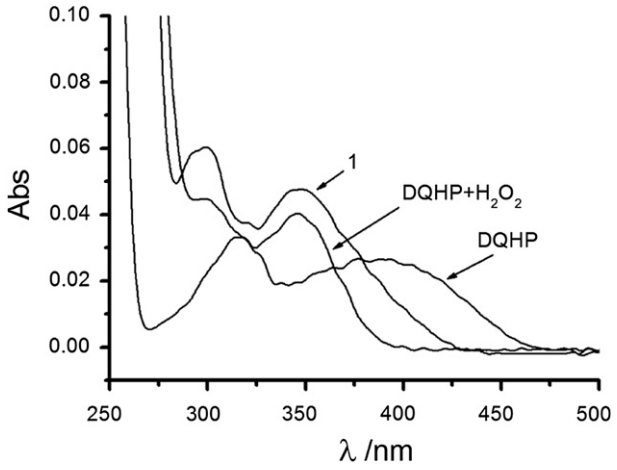

Fig. 2. UV/Vis absorption spectra of DQHP (10 μM), 1 (10 μM), and DQHP (10 μM) with addition of H_2O_2 (1 mM) for 90 min in HEPES buffer (10 mM HEPES, 100 mM NaCl, pH = 7.0).

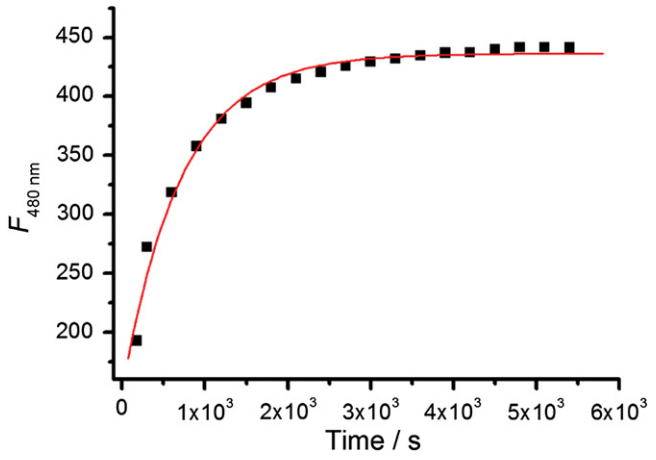

Fig. 4. Time-course kinetic measurement of fluorescence response of DQHP to H_2O_2. Data were collected under pseudo first-order conditions (1.25 μM DQHP, 1 mM H_2O_2) in HEPES buffer. Excitation was provided at 405 nm, and the emission intensities at 480 nm were measured over various time points. Data collected from 3 to 90 min was used to fit the rate constant (red line). (For interpretation of the references to colour in this figure legend, the reader is referred to the web version of this article.)

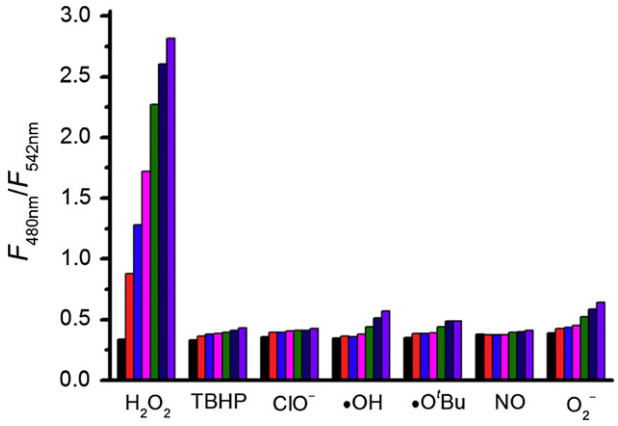

Fig. 5. Fluorescence responses of 5 μM DQHP to various reactive oxygen species (ROS) at 100 μM. Bars represent emission intensity ratios $F_{480}/F_{542\ nm}$ at 5, 15, 30, 60, 90, 120 min after addition of each ROS. Data were acquired at 25 °C in 10 mM HEPES, 100 mM NaCl, pH 7.0, $\lambda_{ex} = 405$ nm.

that halide ions are able to quench the fluorescence of quaternized quinolinium indicators [11], but it is not the case for the probe DQHP. The data show that the fluorescent emission of DQHP is relatively unaffected in the presence of Cl^- (100 mM), Br^- (100 mM) and I^- (10 mM). (Fig. S5).

4. Summary

In summary, we have synthesized and characterized a novel quinoline-based fluorescent probe, DQHP. This probe can detect H_2O_2 through turn-on and ratiometric fluorescence signal output with a significant emission shift. Moreover, the good chemoselectivity for H_2O_2 and pH independence in the biological pH range make DQHP a good candidate for detecting H_2O_2 in aqueous and biological media.

Acknowledgements

We thank the National Basic Research Program of China (No. 2011CB935800), National Natural Science Foundation of China (No. 21102148, 21125205), and the State Key Laboratory of Fine Chemicals, Department of Chemical Engineering, Dalian University of Technology (KF1001) for financial supports.

Appendix A. Supplementary material

Supplementary (additional fluorescence titration data, and NMR spectra associated with this article) data associated with this article can be found, in the online version, at doi:10.1016/j.dyepig.2012.05.013.

References

[1] (a) Finkel T, Serrano M, Blasco MA. The common biology of cancer and ageing. Nature 2007;448:767–74;
(b) Lin MT, Beal MF. Mitochondrial dysfunction and oxidative stress in neurodegenerative diseases. Nature 2006;443:787–95;
(c) Stadtman ER. Protein oxidation and aging. Free Radic Res 2006;40:1250–8;
(d) Sharpless NE, Depinho RA. How stem cells age and why this makes us grow old. Nat Rev Mol Cell Biol 2007;8:703–13.
[2] (a) Balaban RS, Nemoto S, Finkel T. Mitochondria, oxidants, and aging. Cell 2005;120:483–95;
(b) Rhee SG. Cell signaling. H_2O_2, a necessary evil for cell signaling. Science 2006;312:1882–3.
[3] (a) Hempel SL, Buettner GR, O'Malley YQ, Wessels DA, Flaherty DM. Dihydrofluorescein diacetate is superior for detecting intracellular oxidants: comparison with 2′,7′-dichlorodihydrofluorescein diacetate, 5(and 6)-carboxy-2′,7′-dichlorodihydrofluorescein diacetate, and dihydrorhodamine 123. Free Radic Biol Med 1999;27:146–59;
(b) Kim G, Lee YEK, Xu H, Philbert MA, Kopelman R. Nanoencapsulation method for high selectivity sensing of hydrogen peroxide inside live cells. Anal Chem 2010;82:2165–9.
[4] (a) Nagano T. Bioimaging probes for reactive oxygen species and reactive nitrogen species. J Clin Biochem Nutr 2009;45:111–24;
(b) Chen XQ, Tian XZ, Shin I, Yoon JY. Fluorescent and luminescent probes for detection of reactive oxygen and nitrogen species. Chem Soc Rev 2011;40:4783–804;
(c) Wardman P. Fluorescent and luminescent probes for measurement of oxidative and nitrosative species in cells and tissues: progress, pitfalls, and prospects. Free Radic Res 2007;43:995–1022;
(d) Schäferling M, Grögel DBM, Schreml S. Microchim Acta 2011;174:1–18.
[5] Abo M, Urano Y, Hanaoka K, Terai T, Komatsu T, Nagano T. Development of a highly sensitive fluorescence probe for hydrogen peroxide. J Am Chem Soc 2011;133:10629–37.
[6] (a) Dickinson BC, Srikun D, Chang CJ. Mitochondrial-targeted fluorescent probes for reactive oxygen species. Curr Opin Chem Biol 2010;14:50–6;
(b) Lippert AR, Van de Bittner GC, Chang CJ. Boronate oxidation as a bioorthogonal reaction approach for studying the chemistry of hydrogen peroxide in living systems. Acc Chem Res 2011;44:793–804.
[7] Dunn KW, Mayor S, Myers JN, Maxfield FR. Applications of ratio fluorescence microscopy in the study of cell physiology. FASEB J 1994;8:573–82.
[8] (a) Albers AE, Okreglak VS, Chang CJ. A FRET-based approach to ratiometric fluorescence detection of hydrogen peroxide. J Am Chem Soc 2006;128:9640–1;
(b) Srikun D, Miller EW, Domaille DW, Chang CJ. An ICT-based approach to ratiometric fluorescence imaging of hydrogen peroxide produced in living cells. J Am Chem Soc 2008;130:4596–7;
(c) Chung C, Srikun D, Lim CS, Chang CJ, Cho BR. A two-photon fluorescent probe for ratiometric imaging of hydrogen peroxide in live tissue. Chem Commun 2011;47:9618–20;
(d) Markvicheva KN, Bilan DS, Mishina NM, Gorokhovatsky AY, Vinokurov LM, Lukyanov S, et al. A genetically encoded sensor for H_2O_2 with expanded dynamic range. Bioorg Med Chem 2011;19:1079–84;
(e) Masanta G, Heo CH, Lim CS, Bae SK, Cho BR, Kim HM. A mitochondria-localized two-photon fluorescent probe for ratiometric imaging of hydrogen peroxide in live tissue. Chem Commun ASAP, DOI: 10.1039/C2CC00034B.
[9] (a) Dega-Szafran Z, Kania A, Nowak-Wydra B, Szafran M. UV, ^1H and ^{13}C NMR spectra, and AM1 studies of protonation of aminopyridines. J Mol Struct 1994;322:223–32;
(b) Chou P, Wei C. Photophysics of 10-hydroxybenzo[h]quinoline in aqueous solution. J Phys Chem 1996;100:17059–66;
(c) Panda D, Ghosh D, Datta A. Acid–base behavior of 3-aminoquinoline in its ground and excited states. J Photochem Photobiol A 2009;207:254–9;
(d) Xue L, Li GP, Liu Q, Wang HH, Liu C, Ding XL, et al. Ratiometric fluorescent sensor based on inhibition of resonance for detection of cadmium in aqueous solution and living cells. Inorg Chem 2011;50:3680–90;
(e) Xue L, Li GP, Yu CL, Jiang H. A ratiometric and targetable fluorescent sensor for quantification of mitochondrial zinc ions. Chem Eur J 2012;18:1050–4.
[10] Miller EW, Albers AE, Pralle A, Isacoff EY, Chang CJ. Boronate-based fluorescent probes for imaging cellular hydrogen peroxide. J Am Chem Soc 2005;127:16652–9.
[11] Urbano E, Offenbacher H, Wolfbeis OS. Anal Chem 1984;56:427–9.